# Non-contact, portable and stand-off infrared thermal imager for security scanning applications

WeeLiam Khor[1], Yichen Kelly Chen[2], Michael Roberts[2,3], Francesco Ciampa[1†]

[1]Department of Mechanical Engineering Sciences, University of Surrey, Guildford, GU2 7XH, United Kingdom.

[2]Department of Applied Mathematics and Theoretical Physics, University of Cambridge, Wilberforce Road, Cambridge, CB3 0WA, United Kingdom.

[3]Department of Medicine, University of Cambridge, Hills Road, Cambridge, CB2 2QQ, United Kingdom.

[†]Corresponding author: f.ciampa@surrey.ac.uk

## Abstract

In this article, we demonstrated the physical application of a portable infrared (IR) security scanning system for the non-contact and stand-off detection of target objects concealed underneath clothing. Such a system combines IR imaging and transfer learning with convolutional neural network (CNN) to enhance the detection of weak thermal signals and automate the classification of IR images. A mid-wavelength IR detector was used to record the real-time heat emitted from the clothing surface by human subjects. Concealed objects reduce transmissivity of IR radiation from the body to the clothing surface, generally showing lower IR intensity compared to regions without objects. Due to limited resource for training data, the transfer learning approach was applied by fine tuning a pre-trained CNN ResNet-50 model using the ImageNet database. Two image types were here investigated, i.e., raw thermal and Fuzzy-c clustered images. Receiver operating characteristic curves were built using a holdout set, showing an area-under-the-curve of 0.8934 and 0.9681 for the raw and Fuzzy-c clustered image models, respectively. The Gradient-weighted Class Activation Mapping (Grad-CAM) visualisation method was used to improve the target identification, showing accurate prediction of the object area. It was also found that complex clothing, such as those composed of materials of different transmissivity, could mislead the model in classification. The proposed IR-based detector has shown potentials as a non-contact, stand-off security scanning system that can be deployed in diverse locations and ensure higher safety of civilians.

# 1. Introduction

Weapons and IEDs are a common and growing threat to the civilian society and military operations. They are generally used by criminals, terrorists and suicide bombers and may be packed with additional components such as glass, hazardous materials or metal fragments to increase the amount of shrapnel propelled by the explosion [1-6]. Since IEDs are improvised, they can come in many forms, ranging from a small pipe bomb to sophisticated devices capable of causing massive damage and loss of life. Military checkpoints and public spaces such as transport hubs, government buildings, shopping centers and entertainment venues represent high profile targets, such as the recent terrorist attack at the Manchester Arena in 2017 [7].

There is an ongoing need for sensitive and efficient screening systems for the detection of threatening objects concealed underneath people's clothing. Standoff detection is particularly concerned, as it enables security professionals to react to an alarm before the person reaches a check point or entrance. It is also very convenient for people being scanned because in general they do not have to stop their journey and divest [8]. Standoff detection is traditionally divided into two types, bulk and trace. In bulk detection a macroscopic amount of IEDs is detected via imaging technology. In trace detection, instead, microscopic amounts of explosive material in the form of vapor (or particulates) are detected using chemical sensors [8-10]. However, trace detection with optical spectrometry is made difficult by the small amount of material available for sampling. Typical vapor concentrations of volatile explosives (e.g., nitroglycerine) are nearly one part per million at room temperature, and the emanating vapor plume normally contains a substantially lower concentration depending on how the explosive is packaged and stored. Hence, vapor densities can be difficult to detect even with close proximity so that detection at standoff distances is evidently more difficult [9].

Some of the established electromagnetic (EM) waves used in security scanning include X-ray, millimeter-waves (MMW) and terahertz [8]. X-ray imaging systems are used as airport security scanners, which emits X-rays that are short in wavelength ($10^{-7}$ m to $10^{-9}$ m), high in frequency ($3 \times 1016$ Hz to $3 \times 1019$ Hz) and energy (124 keV to 145 eV) [11]. However, X-rays rely on high energy ionizing radiation that is potentially harmful to humans [12-16]. Microwave-based screening devices have been used for detecting concealed target objects. Nevertheless, microwave bi-dimensional magnitude images reveal the body image in full details, thus causing privacy concerns [17]. MMW scanners with 35 GHz, 94 GHz, and 500 GHz typical frequencies are currently used as commercial stand-and-scan detectors at government buildings and airport security checkpoints [18-20]. However, stand and scan MMW systems are complex devices that require fixed infrastructures and the person to stop and pose whilst the scan takes place, which is not very practical for some concepts of operation [21].

Infrared (IR) scanners create thermal images of the natural heat signature emitted by human bodies, without having to expose the subject to any amount of radiation. The efficacy of IR systems as security scanners have shown various level of success [1, 21-28]. IR operates at a shorter wavelength (760 nm to 50 μm) and higher frequency (up to 214 THz) compared to MMW systems. A major challenge for IR imaging technology is the short wavelength compared to MMW systems, where signal

penetration was found to increase with wavelength [29]. For this reason, IR imagers have been used for security scanning purposes only with thin clothing, due to the lack of penetration of thermal signals through layered clothing [21].

Despite physical constraints, there are inherent benefits associated with the utilization of IR systems for security scanning. In comparison to MMW, IR possesses a shorter wavelength, enabling the creation of higher-resolution visual images, thereby facilitating detection from greater distances [1, 30]. It also enables scalability in applications where a larger number of individuals can be captured within broader fields of view. Furthermore, facial images obtained through passive IR imagers are challenging to identify, thus supporting privacy protection [24].

Therefore, owing to concealed object scanning, most of the research has leaned toward MMW or THz technology due to their superior penetration capabilities. While IR has seen less exploration in this particular domain, machine learning methods have proven effective in handling IR data, such as in non-destructive damage assessment and the segmentation of moving objects [31-36]. In an ideal scenario, considerations made after scanning a subject whether a target object is present or not should be both conclusive and precise. However, the constrained penetration capabilities of IR systems can pose challenges for operators in maintaining consistent decision-making, especially when dealing with individuals wearing layered clothing.

To tackle this challenge, an approach is suggested in this context, which involves the incorporation of transfer learning with convolutional neural networks (CNN) for the detection and classification of concealed objects. CNNs are a class of deep learning network architectures that can be applied to the classification of audio, time-series, signals, and most commonly for image classification. In the case of image classification, the input image is passed through layers of convolutional filters, activation functions, pooling layers, and classification layers.

In small dataset problems, the transfer learning approach is typically applied to overcome the shortage of training data. The fundamental idea of the transfer learning approach is that the generic features extracted from an extensive dataset can be both present and informative in diverse datasets. This transferability of learned generic features represents a distinctive advantage of deep learning, i.e., rendering it valuable for a wide array of domain-specific tasks, even when dealing with limited datasets [37]. Leveraging the concept of transfer learning, a pre-existing CNN model can be fine-tuned using data specific to the application. Transfer learning has shown success in various applications, i.e. agricultural pest and disease management [38, 39], image enhancement [40], topology segmentation [41], biomedical imaging [42-46], non-destructive testing in buildings [47], pedestrian identification [48], and security scanning [11, 29].

In image analysis, information reduction by clustering, such as Fuzzy-c [31, 49] can be useful. Data clustering gives distinct cut-offs in the spectrum of continuous values, which in images can allow certain features to be highlighted. Fuzzy-c is an unsupervised machine learning technique, where cluster centers are first established before the cluster affiliation is assigned.

Next, the process involves the calculation of membership scores through distance measurements, revealing the extent of correlation between individual pixels and

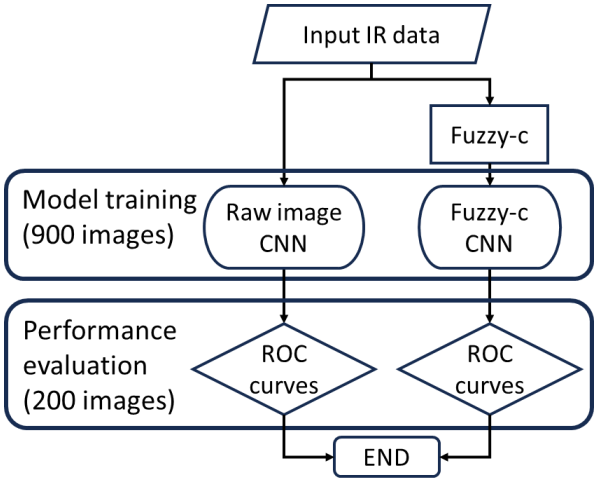


***Figure 1*** *Flowchart for image processing, training, and evaluation of CNN.*

each cluster. These scores then inform the adaptation of cluster centers, with higher emphasis placed on pixels displaying a higher degree of association. This iterative process persists until a predetermined stopping criterion is met.

The purpose of this letter is to investigate the viability of CNN and IR imaging to reveal the presence of hidden objects concealed beneath layered clothing. The study compared the performance of raw IR images and Fuzzy-c clustered images for the fine-tuning of a pre-existing ResNet-50 CNN model. Subsequently, the study assessed the model's performance using the receiver-operating-characteristic (ROC) curves and examined the interpretability of the model's predictions via the Gradient-weighted Class Activation Mapping (Grad-CAM) visualisation method. The flowchart to model training and evaluation is shown in Figure 1.

## 2. Methods

For the collection of IR data, a FLIR A6750sc Mid Wavelength IR camera (waveband between 3 and 5 µm, thermal sensitivity< 20 mK, and 640 × 512 pixels resolution) was used. A selection of objects simulating IED and outer clothing were used in data collection. Some samples of concealed objects and clothing material are shown Figure 2.

For the classification practice, two image types were compared: raw data from the IR camera, and Fuzzy-c clustered images with the cropped region-of-interest (ROI). This intends to examine how the effects of clustering and the removal of non-deterministic information (i.e., background removal) may impact the performance of the trained CNN model in classification. An example of raw image with 256 intensity values is shown in Figure 3(a).

(a) (b) (c)

***Figure 2*** *Photographs of simulated concealed weapons including (a) a vest with pockets of cast iron blocks, and (b) a leather bag with metal ball bearings. Figure (c) illustrates an example of outer clothing tested during the experimental campaign, i.e., a layered windproof jacket.*

The thermal intensity data was transformed into a 1D format prior to processing the pixel intensities using the Fuzzy-c clustering algorithm. A total of 16 cluster centers were defined to represent a total of 16 intensity bins in every image. Fuzzy-c uses a soft clustering technique, allowing each data point to be associated with all available clusters while assigning unique degrees of significance or weighting [50]. Cluster centers were calculated for each iteration until there were no improvement in the objective

function, or if the stopping criteria was achieved. An example of ROI cropped Fuzzy-c clustered image with 16 intensity values is shown in Figure 3(b). Commercial numerical computing software, MATLAB [51] was used for image processing, the training of models, and the analysis of model prediction using Grad-CAM.

ResNet-50 [52] was used as the CNN of choice for IR image classification. Traditionally, when training a CNN model from the ground up, the common recommendation is to have a training dataset that is at least an order of magnitude larger than the test dataset to enhance diversity and prevent overfitting [53, 54]. Nevertheless, well-annotated IR datasets for subjects with concealed objects are infrequent and are frequently not made publicly available. To address the issue of a limited dataset, a publicly available ResNet-50 model pre-trained using the ImageNet dataset [55] was employed in this study. The ImageNet dataset is comprised of 1.4 million images of various natural objects distributed across 1000 classes. For the transfer learning, the fully connected layer was fine-tuned using IR images collected in this work. A total of 900 labelled images, consisting of 462 images with and 438 images without concealed object was used to train models. The fully connected layer was trained using a weight learn rate factor and bias learn rate factor of 10.

Image argumentation, such as transformation by reflection, rotation, and rescaling were applied on to the training images to improve the diversity of data and avoid overfitting. For each training iteration, 30% of randomly sampled training were used for internal validation. Stochastic gradient descent was used as the optimizer with an initial learning rate of 0.0001, validation frequency of 5, maximum epoch of 20 and a mini batch size of 10. Validation accuracies of 98.95% and 95.19% were obtained for the raw image, and ROI cropped Fuzzy C image models respectively.

For the evaluation of model performance, a holdout set with 256 images (equal split of classes) was processed into the raw image

(a) (b)

***Figure 3*** *An example of the dataset image, showing (a) the raw image and (b) the ROI cropped Fuzzy-c clustered image.*

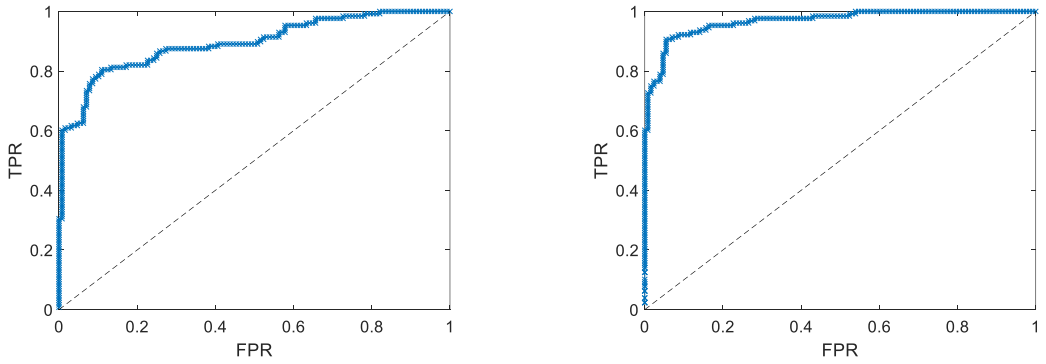


(a) (b)

***Figure 4*** *Receiver operating characteristic (ROC) curves for the model trained using (a) raw images and (b) ROI cropped Fuzzy-c clustered images.*

and Fuzzy-c clustered image types. After classification prediction of the holdout set using the corresponding fine-tuned ResNet-50 models, a confusion matrix labelling of the holdout dataset can be performed by the application of cut-offs on the predicted values. Labelling the prediction into true labels (true positive

and true negative) and false labels (false positive and false negative) will enable the construction of the ROC curve. The ROC curve is a 2D diagram that is built using the True Positive Rate (TPR, also described as sensitivity or recall) and False Positive Rate (FPR, also described as false alarm rate) calculated using the equations given by,

$$TPR = \frac{\Sigma TP}{\Sigma(TP+FN)}, \quad (1a)$$

$$FPR = \frac{\Sigma FP}{\Sigma(FP+TN)}. \quad (1b)$$

The performance of the model is evaluated by the integration of the area-under curve, AUC. The AUC parameter serves as a performance metric for the models: 0.5 suggests no discrimination, 0.7-0.8 is considered acceptable, 0.8-0.9 is considered excellent, and > 0.9 is outstanding [56].

# 3. Result and discussion

ROC curves built using the holdout sets are illustrated in Figure 4, showing an AUC of 0.8934 and 0.9681 for the raw image model and ROI cropped Fuzzy-c clustered image model. Results shows that the ROI Fuzzy-c pre-processed images outperformed the raw images. This is likely due to factors such as the removal of non-deterministic data (background information) and highlighting of the concealed object area (clustering).

The models were trained using images comprising of different clothing material and concealed objects, and therefore it was unsure what specific features were used by the model for classification prediction. The Grad-CAM method was applied to test images and provide a visual explanation to the classification association produced by the model [37, 47, 57-59]. Two images with concealed object were processed using the Grad-CAM method, which are illustrated in Figure 4 alongside the associated visual correspondence and hidden object. On the blue jacket [Figure 5(c)], the model correctly predicted the hidden leather bag with metal ball bearings, which was located around the mid-lower torso area [Figure 5(a)]. On the grey-black jacket [Figure 5(d)], the model mistakenly predicted the hidden weighted vest, where the object was

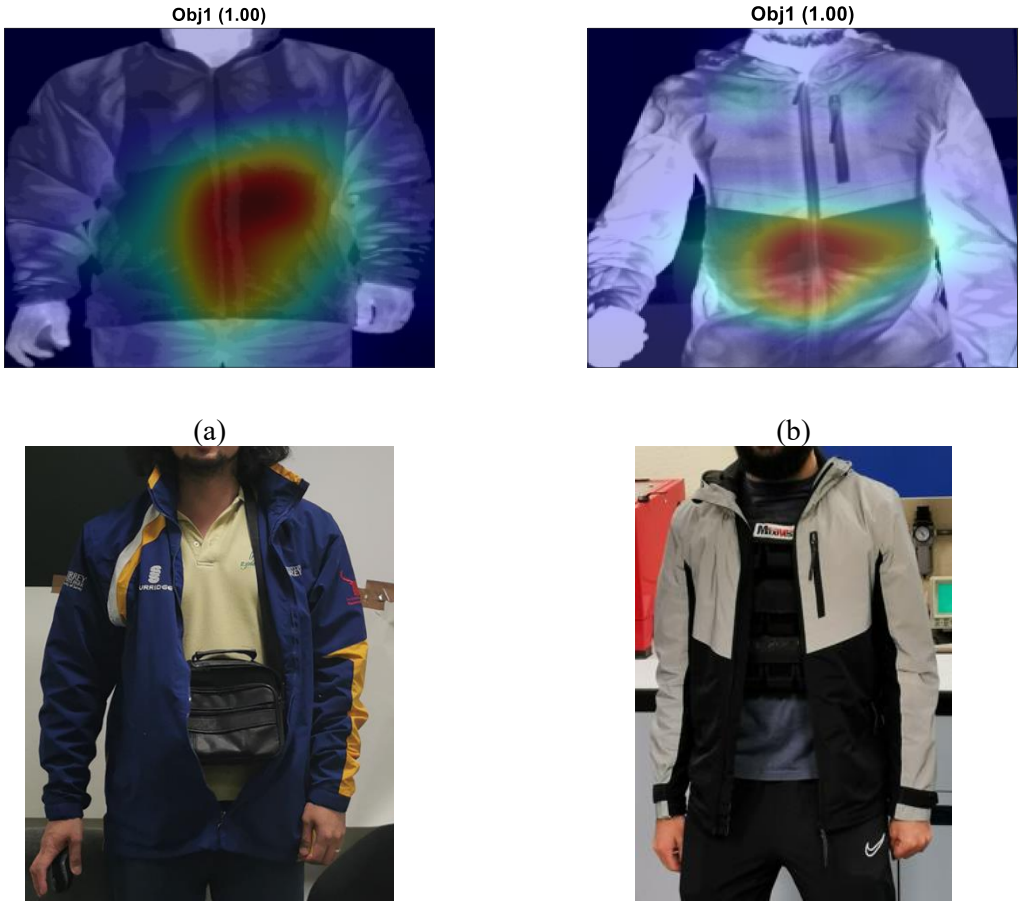


***Figure 5*** *Illustration of the Grad-CAM interpretation of the classification features utilized by the ResNet-50 models [(a) and (b)], and photographs revealing the object location underneath clothing [(c) and (d)].*

predicted to be in the lower torso instead of the upper torso [Figure 5(b)]. In the blue jacket, the layers were consistent across the whole clothing, considering similar transmission across layer, thus allowing the heat trapped by the concealed object to be visualized from the surface of the clothing. However, on the grey-black jacket, the grey region was comparatively smoother than the black region, leading to higher thermal transmission compared to the black layer on the clothing [60-62]. Due to the higher thermal transmission in the grey region, a higher apparent temperature was measured from the IR camera, a step different from the rougher black region surface. Although the model classified the grey-black jacket image correctly, a wrong feature was used due to the complicated design of clothing material.

# 4. Conclusion

The results from this research found that infrared thermography shows potential as an automatic scanner for concealed objects under clothing. Through the application of the transfer learning approach, models showed good classification performance. The Fuzzy-c clustered image model revealed better performance compared to the raw image model. Image pre-processing by information reduction, i.e., Fuzzy-c, removed background data and emphasized the temperature contrast around the object area. Aside from cases of complicated clothing structures (i.e., clothing comprising layers of distinctly different

transmission properties), the Grad-CAM method showed that the model was able to predict the areas of concealed objects effectively.

**Acknowledgements**: Authors acknowledge funds provided by the UK Defense Science and Technology Laboratory (DSTL) through the Defense and Security Accelerator for the IR SCREEN project. Technical support provided by Ian Jupp from DSTL and Colin Cameron from QinetiQ was much appreciated.

**Funding**: This work was supported by the UK Defense and Security Accelerator [grant number ACC2022360].

**Conflict of interest statement**: The authors have no conflicts to disclose.

**Data availability statement**: Trained CNN models and several processed IR images are available for anyone interested in 'testing' the model. Data availability is upon contacting the corresponding author, as the data should not be publicly shared due to the nature of the project.

**Reference:**

[1] J. Binstock and M. Minukas, "Developing an Operational and Tactical Methodology for Incorporating Existing Technologies to Produce the Highest Probability of Detecting an Individual Wearing an IED," Masters, Naval Postgraduate School, Monterey, California, 2010. [Online]. Available: https://www.hsdl.org/c/view?docid=461606

[2] R. F. Ellis, R. D. Rogers, and B. M. Cochran, "Joint Improvised Explosive Device Defeat Organization (JIEDDO): Tactical Successes Mired in Organizational Chaos; Roadblock in the Counter-IED Fight," National defence Univ Norfolk VA Joint Forces Staff Coll, 2007. [Online]. Available: https://apps.dtic.mil/sti/citations/ADA473109

[3] M. A. Ramasamy *et al.*, "Outcomes of IED Foot and Ankle Blast Injuries," *JBJS,* vol. 95, no. 5, 2013. [Online]. Available: https://journals.lww.com/jbjsjournal/fulltext/2013/03060/outcomes_of_ied_foot_and_ankle_blast_injuries.14.aspx.

[4] D. M. Sheen, D. L. McMakin, and T. E. Hall, "Chapter 9 - Detection of Explosives by Millimeter-wave Imaging," in *Counterterrorist Detection Techniques of Explosives*, J. Yinon Ed. Amsterdam: Elsevier Science B.V., 2007, pp. 237-277.

[5] J. E. Sherwood *et al.*, "Multi-drug resistant Bacteroides fragilis recovered from blood and severe leg wounds caused by an improvised explosive device (IED) in Afghanistan," *Anaerobe,* vol. 17, no. 4, pp. 152-155, 2011/08/01/ 2011, doi: https://doi.org/10.1016/j.anaerobe.2011.02.007.

[6] C. Wilson, "Improvised Explosive Devices (IEDs) in Iraq and Afghanistan: Effects and Countermeasures," Library of Congress Washington DC Congressional Research Service, 2007. [Online]. Available: https://apps.dtic.mil/sti/citations/ADA475029

[7] J. Saunders, "Manchester Arena Inquiry - Volume 1: Security for the Arena," in "Report of the Public Inquiry into the Attack on Manchester Arena on 22nd May 2017," 2021. [Online]. Available: https://manchesterarenainquiry.org.uk/report-volume-one/#2

[8] National Research Council, "Existing and Potential Standoff Explosives Detection Techniques," (in English), p. 148, 2004, doi: 10.17226/10998.

[9] J. E. Parmeter, "The challenge of standoff explosives detection," in *38th Annual 2004 International Carnahan Conference on Security Technology, 2004.*, 11-14 Oct. 2004 2004, pp. 355-358, doi: 10.1109/CCST.2004.1405418.

[10] *Innovations in Defence Support Systems - 2 - Socio-Technical Systems*, 1 ed. (Studies in Computational Intelligence). Berlin, Heidelberg: Springer Berlin, Heidelberg, 2011, pp. XIII, 286.

[11] S. Akçay, M. E. Kundegorski, M. Devereux, and T. P. Breckon, "Transfer learning using convolutional neural networks for object classification within X-ray baggage security imagery," in *2016 IEEE International Conference on Image Processing (ICIP)*, 25-28 Sept. 2016 2016, pp. 1057-1061, doi: 10.1109/ICIP.2016.7532519.

[12] H. D. Barth, M. E. Launey, A. A. MacDowell, J. W. Ager, and R. O. Ritchie, "On the effect of X-ray irradiation on the deformation and fracture behavior of human cortical bone," *Bone,* vol. 46, no. 6, pp. 1475-1485, 2010/06/01/ 2010, doi: https://doi.org/10.1016/j.bone.2010.02.025.

[13] H. D. Barth, E. A. Zimmermann, E. Schaible, S. Y. Tang, T. Alliston, and R. O. Ritchie, "Characterization of the effects of x-ray irradiation on the hierarchical structure and mechanical properties of human cortical bone," *Biomaterials,* vol. 32, no. 34, pp. 8892-8904, 2011/12/01/ 2011, doi: https://doi.org/10.1016/j.biomaterials.2011.08.013.

[14] R. L. Brent, "The effect of embryonic and fetal exposure to x-ray, microwaves, and ultrasound: counseling the pregnant and nonpregnant patient about these risks," (in eng), *Semin Oncol,* vol. 16, no. 5, pp. 347-368, 1989/10// 1989. [Online]. Available: http://europepmc.org/abstract/MED/2678486.

[15] K. Faraj and S. Mohammed, "Effects of chronic exposure of X-ray on hematological parameters in human blood," *Comparative Clinical Pathology,* vol. 27, no. 1, pp. 31-36, 2018/01/01 2018, doi: 10.1007/s00580-017-2547-7.

[16] X. Liang, J. Y. Zhang, I. K. Cheng, and J. Y. Li, "Effect of high energy X-ray irradiation on the nano-mechanical properties of human enamel and dentine," *Brazilliam Oral Research,* vol. 30, no. 9, 2016 doi: https://doi.org/10.1590/1807-3107BOR-2016.vol30.0009.

[17] S. Wallin, A. Pettersson, H. Östmark, and A. Hobro, "Laser-based standoff detection of explosives: a critical review," *Analytical and Bioanalytical Chemistry,* vol. 395, no. 2, pp. 259-274, 2009/09/01 2009, doi: 10.1007/s00216-009-2844-3.

[18] C. D. Haworth, Y. De Saint-Pern, D. Clark, E. Trucco, and Y. R. Petillot, "Detection and Tracking of Multiple Metallic Objects in Millimetre-Wave Images," *International Journal of Computer Vision,* vol. 71, no. 2, pp. 183-196, 2007/02/01 2007, doi: 10.1007/s11263-006-6275-8.

[19] C. D. Haworth, Y. De Saint-Pern, Y. R. Petillot, and E. Trucco, "Public security screening for metallic objects with millimetre-wave images," *IET Conference Proceedings,* pp. 1-4. [Online]. Available: https://digital-library.theiet.org/content/conferences/10.1049/ic_20050060

[20] C. Haworth *et al.*, *Image analysis for object detection in millimetre-wave images* (European Symposium on Optics and Photonics for Defence and Security). SPIE, 2004.

[21] N. Jasim Hussein, F. Hu, and F. He, "Multisensor of thermal and visual images to detect concealed weapon using harmony search image fusion approach," *Pattern Recognition Letters,* vol. 94, pp. 219-227, 2017/07/15/ 2017, doi:

https://doi.org/10.1016/j.patrec.2016.12.011.

[22] M. R. Dickson, "Handheld Infrared camera use for suicide bomb detection: feasibility of use for thermal model comparison," Master of Science, Department of Mechanical and Nuclear Engineering, Kansas State University, Manhattan, Kansas, 2008. [Online]. Available: https://krex.k-state.edu/handle/2097/1045

[23] M. Kowalski, M. Kastek, M. Piszczek, M. Życzkowski, and M. Szustakowski, *Harmless screening of humans for the detection of concealed objects*. 2015.

[24] M. Kowalski, A. Grudzień, N. Palka, and M. Szustakowski, *Face recognition in the thermal infrared domain* (SPIE Security + Defence). SPIE, 2017.

[25] M. Kowalski, M. Kastek, and M. Szustakowski, "Concealed Objects Detection in Visible, Infrared and Terahertz Ranges," *International Journal of Computer, Information, Systems and Control Engineering,* vol. 8, pp. 1632-1627, 12/12 2014.

[26] M. Kastek, M. Kowalski, H. Polakowski, P. Lagueux, and M.-A. Gagnon, *Passive signatures concealed objects recorded by multispectral and hyperspectral systems in visible, infrared and terahertz range* (SPIE Defense + Security). SPIE, 2014.

[27] M. Kowalski, M. Kastek, N. Palka, H. Polakowski, M. Szustakowski, and M. Piszczek, "Investigations of concealed objects detection in visible, infrared and terahertz ranges," *Photonics Letters of Poland,* vol. 5, pp. 167-169, 12/31 2013, doi: 10.4302/plp.2013.4.16.

[28] C. Corsi, "Infrared: A Key Technology for Security Systems," in *Sensors*, New York, NY, F. Baldini *et al.*, Eds., 2014// 2014: Springer New York, pp. 37-42.

[29] M. Kowalski, "Real-time concealed object detection and recognition in passive imaging at 250GHz," *Appl. Opt.,* vol. 58, no. 12, pp. 3134-3140, 2019/04/20 2019, doi: 10.1364/AO.58.003134.

[30] N. Kukutsu and Y. Kado, "Overview of Millimeter and Terahertz Wave Application Research," *NTT Technical Review,* vol. 7, no. 3, 2009. [Online]. Available: https://www.ntt-review.jp/archive/ntttechnical.php?contents=ntr200903sf1.html#top.

[31] Z. Wang, L. Wan, N. Xiong, J. Zhu, and F. Ciampa, "Variational level set and fuzzy clustering for enhanced thermal image segmentation and damage assessment," *NDT & E International,* vol. 118, p. 102396, 2021/03/01/ 2021, doi: 10.1016/j.ndteint.2020.102396.

[32] Z. Wang, J. Zhu, G. Tian, and F. Ciampa, "Comparative analysis of eddy current pulsed thermography and long pulse thermography for damage detection in metals and composites," *NDT & E International,* vol. 107, p. 102155, 2019/10/01/ 2019, doi: 10.1016/j.ndteint.2019.102155.

[33] D. Wang, Z. Wang, J. Zhu, and F. Ciampa, "Enhanced pre-processing of thermal data in long pulse thermography using the Levenberg-Marquardt algorithm," *Infrared Physics & Technology,* vol. 99, pp. 158-166, 2019/06/01/ 2019, doi: 10.1016/j.infrared.2019.04.009.

[34] Z. Wang, G. Tian, M. Meo, and F. Ciampa, "Image processing based quantitative damage evaluation in composites with long pulse thermography," *NDT & E International,* vol. 99, pp. 93-104, 2018/10/01/ 2018, doi: 10.1016/j.ndteint.2018.07.004.

[35] B. Chen, W. Wang, and Q. Qin, "Robust multi-stage approach for the detection of moving target from infrared imagery," *Optical Engineering,* vol. 51, no. 6, p. 067006, 2012. [Online]. Available: https://doi.org/10.1117/1.OE.51.6.067006.

[36] P. Cotič, Z. Jagličić, E. Niederleithinger, M. Stoppel, and V. Bosiljkov, "Image Fusion for Improved Detection of Near-Surface Defects in NDT-CE Using Unsupervised Clustering Methods," *Journal of Nondestructive Evaluation,* vol. 33, no. 3, pp. 384-397, 2014/09/01

2014, doi: 10.1007/s10921-014-0232-1.

[37] R. Yamashita, M. Nishio, R. K. G. Do, and K. Togashi, "Convolutional neural networks: an overview and application in radiology," *Insights into Imaging,* vol. 9, no. 4, pp. 611-629, 2018/08/01 2018, doi: 10.1007/s13244-018-0639-9.

[38] W. Dawei, D. Limiao, N. Jiangong, G. Jiyue, Z. Hongfei, and H. Zhongzhi, "Recognition pest by image-based transfer learning," *Journal of the Science of Food and Agriculture,* vol. 99, no. 10, pp. 4524-4531, 2019/08/15 2019, doi: https://doi.org/10.1002/jsfa.9689.

[39] I. Z. Mukti and D. Biswas, "Transfer Learning Based Plant Diseases Detection Using ResNet50," in *2019 4th International Conference on Electrical Information and Communication Technology (EICT)*, 20-22 Dec. 2019 2019, pp. 1-6, doi: 10.1109/EICT48899.2019.9068805.

[40] Y. Huang, Z. Jiang, R. Lan, S. Zhang, and K. Pi, "Infrared Image Super-Resolution via Transfer Learning and PSRGAN," *IEEE Signal Processing Letters,* vol. 28, pp. 982-986, 2021, doi: 10.1109/LSP.2021.3077801.

[41] A. Shabbir *et al.*, "Satellite and Scene Image Classification Based on Transfer Learning and Fine Tuning of ResNet50," *Mathematical Problems in Engineering,* vol. 2021, p. 5843816, 2021/07/13 2021, doi: 10.1155/2021/5843816.

[42] J. Hong, H. Cheng, Y.-D. Zhang, and J. Liu, "Detecting cerebral microbleeds with transfer learning," *Machine Vision and Applications,* vol. 30, no. 7, pp. 1123-1133, 2019/10/01 2019, doi: 10.1007/s00138-019-01029-5.

[43] M. Muazzam *et al.*, "Transfer Learning Assisted Classification and Detection of Alzheimer's Disease Stages Using 3D MRI Scans," (in English), *Sensors,* vol. 19, no. 11, 2020-06-12 2019, doi: https://doi.org/10.3390/s19112645.

[44] G. Liang and L. Zheng, "A transfer learning method with deep residual network for pediatric pneumonia diagnosis," *Computer Methods and Programs in Biomedicine,* vol. 187, p. 104964, 2020/04/01/ 2020, doi: https://doi.org/10.1016/j.cmpb.2019.06.023.

[45] H. C. Shin *et al.*, "Deep Convolutional Neural Networks for Computer-Aided Detection: CNN Architectures, Dataset Characteristics and Transfer Learning," *IEEE Transactions on Medical Imaging,* vol. 35, no. 5, pp. 1285-1298, 2016, doi: 10.1109/TMI.2016.2528162.

[46] M. Gezimati and G. Singh, "Transfer Learning for Breast Cancer Classification in Terahertz and Infrared Imaging," in *2022 International Conference on Artificial Intelligence, Big Data, Computing and Data Communication Systems (icABCD)*, 4-5 Aug. 2022 2022, pp. 1-6, doi: 10.1109/icABCD54961.2022.9856138.

[47] Y. Gao and K. M. Mosalam, "Deep Transfer Learning for Image-Based Structural Damage Recognition," *Computer-Aided Civil and Infrastructure Engineering,* vol. 33, no. 9, pp. 748-768, 2018/09/01 2018, doi: https://doi.org/10.1111/mice.12363.

[48] J. Hu, Y. Zhao, and X. Zhang, "Application of Transfer Learning in Infrared Pedestrian Detection," in *2020 IEEE 5th International Conference on Image, Vision and Computing (ICIVC)*, 10-12 July 2020 2020, pp. 1-4, doi: 10.1109/ICIVC50857.2020.9177438.

[49] W. Khor, Y. K. Chen, M. Roberts, and F. Ciampa, "Infrared thermography as a non-invasive scanner for concealed weapon detection," *Defence and Security Doctoral Symposium 2023 (DSDS23),* 2024, doi: https://doi.org/10.17862/cranfield.rd.25028030.v2.

[50] J. C. Bezdek, *Pattern Recognition with Fuzzy Objective Function Algorithms*. Advanced Applications in Pattern Recognition: Springer New York, NY, 1981, p. 272.

[51] The MathWorks Inc, "MATLAB version: 9.12.0 (R2022a)," 2022. [Online].

Available: https://www.mathworks.com.

[52] K. He, X. Zhang, S. Ren, and J. Sun, "Deep Residual Learning for Image Recognition," in *2016 IEEE Conference on Computer Vision and Pattern Recognition (CVPR)*, 27-30 June 2016 2016, pp. 770-778, doi: 10.1109/CVPR.2016.90.

[53] J. T. Barry-Straume, Adam; Engels, Daniel W.; Fine, Edward, "An Evaluation of Training Size Impact on Validation Accuracy for Optimized Convolutional Neural Networks," *SMU Data Science Review,* vol. 1, 2018. [Online]. Available: https://scholar.smu.edu/datasciencereview/vol1/iss4/12.

[54] K. L. Junghwan Cho, Ellie Shin, Garry Choy, Synho Do, "How much data is needed to train a medical image deep learning system to achieve necessary high accuracy?," *ICLR 2016,* 2016 doi: https://doi.org/10.48550/arXiv.1511.06348.

[55] J. Deng, W. Dong, R. Socher, L. J. Li, L. Kai, and F.-F. Li, "ImageNet: A large-scale hierarchical image database," in *2009 IEEE Conference on Computer Vision and Pattern Recognition*, 20-25 June 2009 2009, pp. 248-255, doi: 10.1109/CVPR.2009.5206848.

[56] J. N. Mandrekar, "Receiver Operating Characteristic Curve in Diagnostic Test Assessment," *Journal of Thoracic Oncology,* vol. 5, no. 9, pp. 1315-1316, 2010/09/01/ 2010, doi: https://doi.org/10.1097/JTO.0b013e3181ec173d.

[57] D. Melching, T. Strohmann, G. Requena, and E. Breitbarth, "Explainable machine learning for precise fatigue crack tip detection," *Scientific Reports,* vol. 12, no. 1, p. 9513, 2022/06/09 2022, doi: 10.1038/s41598-022-13275-1.

[58] P. Linardatos, V. Papastefanopoulos, and S. Kotsiantis, "Explainable AI: A Review of Machine Learning Interpretability Methods," *Entropy,* vol. 23, no. 1, p. 18, 2021. [Online]. Available: https://www.mdpi.com/1099-4300/23/1/18.

[59] R. R. Selvaraju, M. Cogswell, A. Das, R. Vedantam, D. Parikh, and D. Batra, "Grad-CAM: Visual Explanations from Deep Networks via Gradient-Based Localization," *International Journal of Computer Vision,* vol. 128, no. 2, pp. 336-359, 2020/02/01 2020, doi: 10.1007/s11263-019-01228-7.

[60] Y. Yu *et al.*, "Effects of surface roughness on terahertz transmission spectra," *Optical and Quantum Electronics,* vol. 52, no. 5, p. 240, 2020/04/27 2020, doi: 10.1007/s11082-020-02365-x.

[61] S. Koshimizu, "Measurement of Surface Roughness and Thickness of Silicon Wafers Using an Infrared Laser," *Key Engineering Materials,* vol. 291-292, pp. 377-380, 2005, doi: 10.4028/www.scientific.net/KEM.291-292.377.

[62] A. Larena, F. Millán, G. Pérez, and G. Pinto, "Effect of surface roughness on the optical properties of multilayer polymer films," *Applied Surface Science,* vol. 187, no. 3, pp. 339-346, 2002/02/28/ 2002, doi: https://doi.org/10.1016/S0169-4332(01)01044-3.